



HAL
open science

Preliminary study of electrochemical conversion of glucose on novel modified nickel electrodes

Erwann Ginoux, Gabriel David Acosta Hidalgo, Patrick Cognet, Yolande Pérès,
Laure Latapie, Lionel Estel, Alain Ledoux

► **To cite this version:**

Erwann Ginoux, Gabriel David Acosta Hidalgo, Patrick Cognet, Yolande Pérès, Laure Latapie, et al.. Preliminary study of electrochemical conversion of glucose on novel modified nickel electrodes. *Journal of Applied Electrochemistry*, In press, pp.2039-2049. <10.1007/s10800-024-02083-2>. <hal-04510236>

HAL Id: hal-04510236

<https://hal.science/hal-04510236v1>

Submitted on 19 Mar 2024

HAL is a multi-disciplinary open access archive for the deposit and dissemination of scientific research documents, whether they are published or not. The documents may come from teaching and research institutions in France or abroad, or from public or private research centers.

L'archive ouverte pluridisciplinaire **HAL**, est destinée au dépôt et à la diffusion de documents scientifiques de niveau recherche, publiés ou non, émanant des établissements d'enseignement et de recherche français ou étrangers, des laboratoires publics ou privés.



HAL Authorization

Preliminary Study of Electrochemical Conversion of Glucose on Novel Modified Nickel Electrodes

Erwann Ginoux^[a], Gabriel Acosta^[a,b], Patrick Cognet^[a], Yolande Pérès^[a], Laure Latapie^[a], Lionel Estel^[b] and Alain Ledoux^[b]

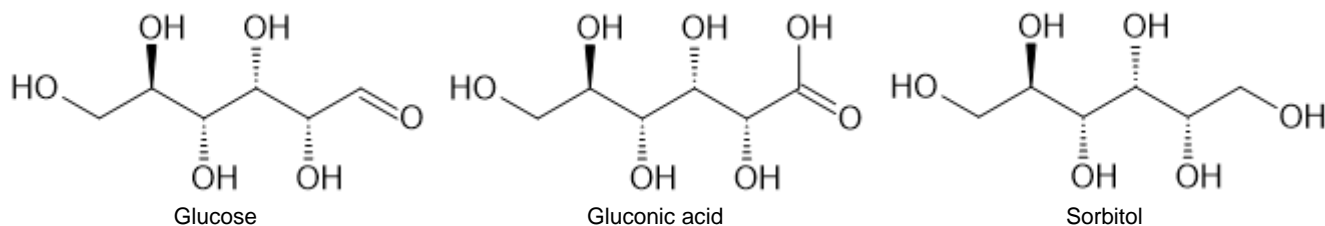
[a] E. Ginoux, G. Acosta, Prof. P. Cognet, Dr. Y. Pérès, L. Latapie
Science et Technique des Procédés Intensifiés
Laboratoire de Génie Chimique LGC
4 Allée Emile Monso, 31030 Toulouse
E-mail: erwann.ginoux@toulouse-inp.fr, gabriel.acosta@insa-rouen.fr, patrick.cognet@toulouse-inp.fr

[b] Prof. Lionel Estel, Dr. Alain Ledoux
Laboratoire de Sécurité des Procédés Chimiques LSPC
INSA Rouen, Avenue de l'université, 76800 Saint-Etienne du Rouvray

Abstract: Gluconic acid and sorbitol are among the value-added chemicals that can be derived from biomass. While these compounds are typically produced through biotechnological processes, electrochemical methods offer numerous advantages over alternative approaches. While studies have extensively explored metals like copper, palladium, gold, and platinum, nickel has received relatively limited attention in this context. Notably, nickel exhibits electrochemical activity suitable for organic electrosynthesis. This work has been achieved with 5 hours long-term electrolysis, glucose as a reactant, utilizing modified nickel electrodes in a KOH solution. While these studies achieved substantial conversion rates, the selectivities and Faraday efficiencies toward gluconic acid and sorbitol remained comparatively low. The long-term electrolysis of glucose using modified nickel electrodes resulted in the identification of various side products. These include formic acid, oxalic acid, glycolic acid, tartronic acid, glyceric acid, and arabinose.

Introduction

Gluconic acid (GA) and sorbitol (S) (Figure 1) are part of the top-30 list of value-added chemicals derived from biomass^{[1], [2]}. They are typically used in numerous industries, including food, pharmaceuticals, cosmetics, and the construction industry. Both the gluconic acid and sorbitol markets are projected to continuously grow in the coming decades^{[3], [4]}. Gluconic acid is currently obtained through the transformation of glucose (Figure 1) using biotechnological methods^[5]. While this technique offers many advantages, it also has some disadvantages, such as slow conversion, complex multicomponent media, a large footprint, and a complicated separation process. These limitations have led to an increased interest in the development of heterogeneous catalytic methods for transforming glucose into value-added products^[6].

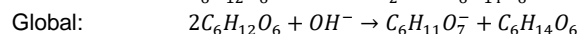
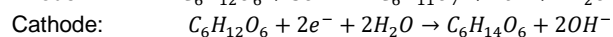
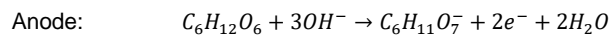


Electrochemical processes offer numerous advantages: they can be associated with heterogeneous catalysis, avoid the use of strong chemical oxidants/reductants, exhibit high tunability and controllability, and are often conducted under mild temperatures and pressures^[7]. A lot of research has been done so far on electrochemical processes using biomass-derived platform molecules^{[8], [9]}, such as the electrooxidation of 5-hydroxymethylfurfural^{[10], [11]}, of glycerol^{[12], [13]}, levulinic acid^{[14], [15]}, glucose and xylose^{[16], [17], [18], [19]} and the electroreduction of 5-hydroxymethylfurfural^{[20], [21]}.

The utilization of electrochemical methods for producing sorbitol and gluconic acid from glucose was developed quite early using graphite anode and Zn(Hg) cathode^[25]. Although sorbitol was industrially produced through an electrochemical process before 1950^[22], the rising electricity prices, coupled with insufficient development of electrochemical technologies and environmental concerns, led to the replacement of the electrochemical technology with a heterogeneous catalytic process using Raney Ni catalyst. Nevertheless, the recent growth in renewable electricity production over the last decade has renewed interest in electrochemical methods for biomass conversion^{[23], [24]}.

Recent developments in electrocatalysis have led to increased energy efficiency and selectivity in electro-organic processes, achieved by utilizing electrocatalytic materials to reduce anode and cathode overpotentials. This advancement has also contributed to a more favourable environmental footprint by replacing less eco-friendly materials, such as mercury electrodes used in the past. Furthermore, the oxidation and reduction of glucose can be combined within a single cell ^{[25], [26]}, enabling the production of value-added products at both the anode and cathode, a rarity in such processes.

In this study, both electrodes, operating with an alkaline electrolyte, have been employed to generate value-added compounds. Glucose is oxidized at the anode to produce gluconate, while glucose is reduced at the cathode to yield sorbitol. This approach aims to minimize the energy requirements of the process.



The objective of this study is to design a continuous electrochemical reactor that eliminates the need for strategic platinum group metals (PGM), while enabling the simultaneous production of gluconic acid at the anode and sorbitol at the cathode. The electrooxidation of glucose to gluconic acid (and glucaric acid) has been extensively investigated using various metals, such as copper, platinum, and gold ^{[27], [28]}, but nickel has not been explored for this purpose thus far.

To achieve this goal, mono- and bi-metallic Ni-based materials have been utilized as both the anode and cathode. These materials were investigated under well-defined conditions in a three-electrode electrochemical cell, operating in alkaline media. The aim was to attain optimal yields and selectivities for both the electrooxidation and electroreduction of glucose, thereby maximizing the efficiency of the process.

Methods and Experimental Details

Reagents

D-glucose (>99%), Gluconic acid potassium salt (99%), D-fructose (99%), tarttronic acid (Tar. Ac.) (97%), glycolic acid (Gly. Ac.) (99%), oxalic acid (Ox. Ac.) (98%), D-arabinose (Ara) (>99%) and DL-Glyceric acid hemicalcium salt hydrate (Glyce. Ac.) (>98%) were purchased from Sigma Aldrich. Sorbitol (91.5<assay<100.5%) and formic acid (For. Ac.) (98%) were purchased from Fisher Scientific. Potassium hydroxide pellets (85%) was purchased from Honeywell. Sulfuric acid (>95-97%) (used for HPLC mobile phase) was purchased from Merck Millipore. HPLC grade water (Milli-Q system, Millipore) was used for reagents and the HPLC mobile phase.

Experimental Set-up

The electroanalytical study (cyclic voltammetry) was performed with an electrochemical reactor made up of a 100mL cell and a three-electrode setup (an auxiliary electrode, a working electrode and a saturated calomel reference electrode (only for cyclic voltammetry)).

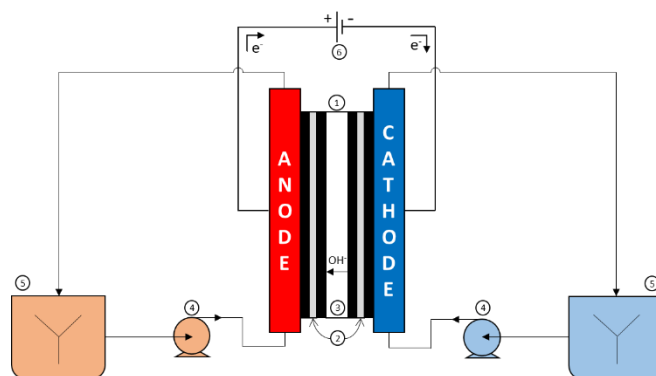


Figure 2. Experimental set up with the electrochemical reactor ①, electrodes ②, membrane ③, peristaltic pumps ④, magnetic stirrers ⑤ and potentiostat ⑥

The electrolyses were performed (Figure 2) with a Micro Flow Cell from ElectroCell (electrode surface area of 10 cm²) (①), both anode and cathode were made of nickel foam purchased from Recemat BV (②) (Table 1) and the reference electrode is an Ag/AgCl 3.4 M KCl made of PTFE (inserted in the cathode compartment). Anodic and cathodic compartments were separated with an anionic exchange membrane AHA from Eurodia (③). Constant flow rates were achieved in each compartment with 2 peristaltic pumps from Masterflex (④) and the feeding solutions were constantly stirred with 2 magnetic stirrers from Masterflex (⑤). Voltage was applied with

77 a Radiometer potentiostat (Ⓢ), assisted by a computer with the software VoltaMaster 2. The electrochemical method
78 chronoamperometry was used to apply a constant potential during electrolysis.

79
80 Since for cyclic voltammetry and electrolysis reference electrodes are not the same, a reference vs RHE will be used to compare
81 potentials with the following equations.

$$E(V \text{ vs. RHE}) = E(V \text{ vs. Ag|AgCl}) + E^\circ(V \text{ vs. Ag|AgCl}) + 0.059 \cdot pH$$

$$E(V \text{ vs. RHE}) = E(V \text{ vs. Ag|AgCl}) + 0.208 + 0.059 \cdot 13$$

$$E(V \text{ vs. RHE}) = E(V \text{ vs. Hg, Hg}_2\text{Cl}_2|\text{Cl}^-) + E^\circ(V \text{ vs. Hg, Hg}_2\text{Cl}_2|\text{Cl}^-) + 0.059 \cdot pH$$

$$E(V \text{ vs. RHE}) = E(V \text{ vs. Ag|AgCl}) + 0.248 + 0.059 \cdot 13$$

87
88 **Table 1.** Nickel foams characteristics

Grade	20 pores cm ⁻¹
Estimated average pore diameter	0.4 mm
Density average	0.3 – 0.6 g cm ⁻³
Relative density (foam / solid Ni)	4.8 %
Porosity	95.2 %
Specific surface	5400 m ² m ⁻³
Specific surface area density	0.079 kg m ⁻²

89
90 **Synthesis of particles on modified nickel electrodes**

91 To crystallize particles on the surface of metal supports, hydrothermal reactions have been employed. This process involves using an
92 aqueous precursor solution at high temperature and pressure to generate fine oxide particles with a size below 100 nm [29]. The reaction
93 components include:

- 94 - a precursor: a metal source in aqueous solution, in our case nickel, cobalt and rhodium salts (Ni(NO₃)₂, RhCl₃.xH₂O, Co(NO₃)₂).
- 95 - a mineralizer to control the solution pH, in our case it is urea.
- 96 - an additive to control particles morphology, in our case, urea.

97 This synthesis took place in an autoclave to surpass the boiling temperature of the solvent. Particle growth resulted from the precursor's
98 solubility in water at the hydrothermal reaction's elevated temperature and pressure. A temperature gradient was maintained within the
99 reactor: the solute dissolved at the highest temperature, while at the lowest temperature, it settled onto the metallic support, leading to
100 particle formation.

101 The pH significantly impacts the size and crystallinity of the particles. Introducing small amounts of ammonium hydroxide [30], ethanol
102 [31], or urea [32] into the precursor solution enhances crystallization kinetics. A typical procedure for manufacturing these particles on
103 nickel foams involved dissolving the precursor, mineralizer, and additive in deionized water. This mixture is then placed into an
104 autoclave with the nickel foams.

105 The autoclave is heated to approximately 100 °C for 8 hours in an electric oven. Subsequently, the electrodes are cooled to room
106 temperature, rinsed with deionized water, and dried at 100-120 °C for 1 hour. Finally, the electrodes underwent calcination at 300 °C
107 for 2 hours [33].

110
111 **Analytical Instruments**

112 After electrolysis, the samples were acidified in order to have a pH around 1-3 (which initially is 13 in the cathodic and anodic media).
113 The samples for the HPLC analyses were diluted 3 times before electrolysis to check initial concentrations and twice after electrolysis
114 in order to have all products concentration between 0.1 g L⁻¹ and 2 g L⁻¹, filtered with a 0.22 μm syringe filter and collected in a 2 mL
115 glass screw-top vial.

116 A Thermo Vanquish HPLC equipped with a Vanquish Split Sampler and an Aminex HPX-87H column (300 x 7.8 mm, 9 μm particle
117 size, 8% cross-linkage, pH range 1-3) was used. Both UV and RI detectors were used: Vanquish Variable Wavelength UV detector
118 allowing up to 4 wavelengths acquisitions at the same time and a refractive index detector (RID) (RefractoMax 520).

119 A 10 mmol/L sulfuric acid solution was used as a mobile phase in isocratic conditions with a flow rate of 0.6 mL min⁻¹. The injection
 120 volume was 20 µL and the column temperature was 50 °C. Separation took about 16 minutes. Sample quantification took place using
 121 external calibration in a range of 0.2 to 2 g L⁻¹ for glucose, gluconic acid, sorbitol, fructose and arabinose and a range of 0.01 to 1 g L⁻¹
 122 for formic acid, glycolic acid, oxalic acid, tartronic acid and glyceric acid.

123 The linearity of the method was checked using 5-6 levels of concentrations (0.2, 0.5, 0.8, 1.2, 1.5 and 2 g L⁻¹ for glucose, gluconic acid,
 124 sorbitol and fructose and 0.01, 0.05, 0.1, 0.4, 0.7 and 1 g L⁻¹ for formic acid, glycolic acid, oxalic acid and tartronic acid) and with 5
 125 independently prepared repetitions per level. All calibrations curves had at minima a regression coefficient (r²) of 0.998 for both UV
 126 (glucose and sorbitol cannot be detected with UV detector) and RI detectors.

127 The conversion X (Equation 1), products yields (Equation 2) and product selectivities (Equation 3) (yield and selectivities were corrected
 128 with a carbon ratio $v_{carbons,product}$ due to the degradation products obtained coming from breaking C-C bonds, indeed selectivities and
 129 faradaic efficiency can reach above 100% if they are not corrected with this carbon ratio; degradation products are obtain via
 130 degradation of glucose but also degradation of bigger degradation products such as a C3 to C2 or C1 product) were then calculated
 131 the following way:

132 **Equation 1.** Glucose conversion equation

$$133 \quad X (\%) = \frac{\text{Amount of glucose converted (C in mole)}}{\text{Amount of glucose in reactant (C in mole)}} \times 100$$

$$134 \quad = \left(1 - \frac{C_{glucose,t}}{C_{glucose,0}} \right) \times 100$$

135 **Equation 2.** Product yield equation

$$136 \quad Y (\%) = \frac{\text{Amount of product formed (C in mole)} v_{carbons,product}}{\text{Amount of glucose in reactant (C in mole)} v_{carbons,glucose}} \times 100$$

$$137 \quad = \left(\frac{C_{product,t}}{C_{glucose,0}} \right) \left(\frac{v_{C,product}}{v_{C,glucose}} \right) \times 100$$

138 **Equation 3.** Product selectivity equation

$$139 \quad S (\%) = \frac{\text{Amount of product (C in mole)} v_{carbons,product}}{\text{Amount of glucose converted (C in mole)} v_{carbons,glucose}} \times 100$$

$$140 \quad = \left(\frac{C_{product,t}}{C_{glucose,0} - C_{glucose,t}} \right) \left(\frac{v_{C,product}}{v_{C,glucose}} \right) \times 100 = \frac{Y}{X}$$

141 Faraday Efficiency

142 To quantify the portion of electricity utilized for each electrochemical reaction, Faraday efficiency is calculated using the following
 143 formula with n_p moles of products p obtained when charge Q is consumed (mol), v_e number of electrons consumed by the
 144 electrochemical reaction, F = 96,500 C mol⁻¹ the Faraday constant, v_p the stoichiometry of the product obtained and Q the charge
 145 consumed (C) (Equation 4):

146 **Equation 4.** Faraday efficiency equation

$$147 \quad \varphi^e = \frac{n_p v_e F}{v_p Q} \text{ with } Q = \int_0^t I dt$$

148 Side products redox reactions

149 Formic acid, glycolic acid, oxalic acid, glyceric acid, tartronic acid and arabinose are obtained from glucose from redox reactions that
 150 imply a specific number of electrons in alkaline medium. Glucose oxidation reactions are written the following way:

151 **Equation 5.** Formic acid formation



153 **Equation 6.** Glycolic acid formation



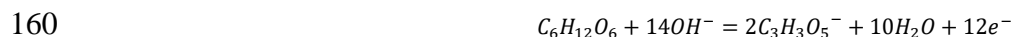
155 **Equation 7.** Oxalic acid formation



157 **Equation 8.** Glyceric acid formation



159 **Equation 9.** Tartronic acid formation



161 **Equation 10.** Arabinose formation



163 At pH 13, all the carboxylic acids are in conjugate base form: formate, glycolate, oxalate, glycerate and tartronate.

164 **Uncertainties**

165 Uncertainties were calculated for glucose conversion, product yields and product selectivities the following way:

166 **Equation 11.** Uncertainty on conversion

$$167 \quad \frac{u(X)}{X} = \sqrt{\left(\frac{u(C_{glucose,0})}{C_{glucose,0}}\right)^2 + \left(\frac{u(C_{glucose,t})}{C_{glucose,t}}\right)^2}$$

168 **Equation 12.** Uncertainty on yield

$$169 \quad \frac{u(Y)}{Y} = \sqrt{\left(\frac{u(C_{product,t})}{C_{product,t}}\right)^2 + \left(\frac{u(C_{product,0})}{C_{product,0}}\right)^2}$$

170 **Equation 13.** Uncertainty on selectivity

$$171 \quad \frac{u(S)}{S} = \sqrt{\left(\frac{u(X)}{X}\right)^2 + \left(\frac{u(Y)}{Y}\right)^2}$$

172 Uncertainties were also calculated for the Faraday efficiency the following way:

173 **Equation 13.** Uncertainty on Faraday efficiency

$$174 \quad \frac{u(\varphi^e)}{\varphi^e} = \sqrt{\left(\frac{u(n_p)}{n_p}\right)^2 + \left(\frac{u(Q)}{Q}\right)^2}$$

175 These uncertainties ^[34] were then multiplied by the coverage factor k (equal to 2 for a confidence interval of 95.5%): $U(x) = 2u(x)$.

176 Repetition of the experiments (each experiment was run 3 times) was factored into the calculation of uncertainties for conversion, yield,
177 and selectivity. The calculation did not incorporate mathematical methods from calibration curves, dilution, or weighing uncertainties.

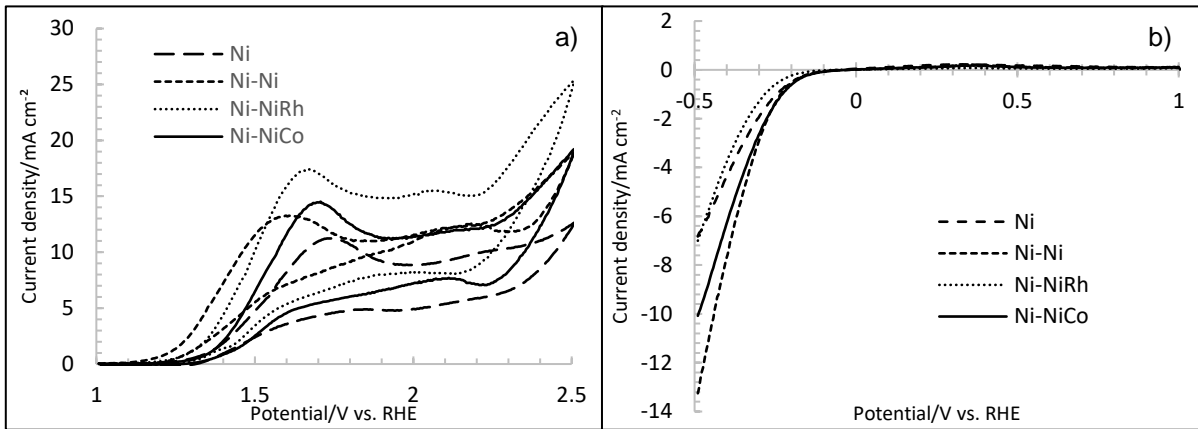
178 **Results and Discussion**

179 **Electroanalytical Results**

180 Three nickel foams with metallic particles (nickel, rhodium and cobalt particles) were analysed electrochemically using cyclic
181 voltammetry. Both oxidation and reduction of glucose were studied on these electrodes, in comparison to pure nickel foam.

182
183
184

Cyclic voltammetry (CV) was used from 1 V to 2.5 V vs. RHE for the oxidation of glucose and from 1 V to -0.5 V vs. RHE, with 0.1 mol L⁻¹ of glucose and KOH, at a sweep rate of 20 mV s⁻¹, to observe the electrochemical activity of these nickel foams with or without metallic particles.



191 **Figure 3.** CV curves of different nickel foam electrodes with NiM particles with 0.1 mol L⁻¹ of glucose and KOH at a sweep rate of 20 mV s⁻¹,
a) for the oxidation part between 1V and 2.5 V vs. RHE, b) for the reduction part between 1V and -0.5 V vs. RHE;

191

192
193
194
195
196
197

Concerning the glucose oxidation (Figure 3a), all electrodes show an electrochemical activity between 1.4 and 1.8 V vs RHE. This current increase reveals the oxidation of glucose into various products. So far, all electrodes with metallic particles express a better electrochemical activity than pure nickel ($j_{\text{Ni-NiRh}} > j_{\text{Ni-NiCo}} > j_{\text{Ni-Ni}} > j_{\text{Ni}}$). However, the Ni-Ni particles allow a lower applied potential to oxidise glucose. Indeed, high voltage potential can lead to break C – C bonds and create degradation products from glucose: indeed, since there is arabinose in the degradation products of glucose in alkaline medium, it is an evidence on the break of C – C bonds of glucose (arabinose has 5 carbons while glucose has 6 carbons).

198
199
200
201
202

Concerning the glucose reduction (Figure 3b), in presence of glucose, no peak is detected as the glucose reduction into sorbitol. The glucose reduction peak is overlapped with the water reduction peak so when sorbitol is produced by glucose reduction, hydrogen is also produced by water reduction. All electrodes show an electrochemical activity between -0.2 V and -0.4 V vs. RHE. But the Ni-Ni electrode seems to have a higher activity than the 2 other electrodes tested ($|j_{\text{Ni-Ni}}| > |j_{\text{Ni-NiCo}}| > |j_{\text{Ni}}|$). This difference of current is referring to Hydrogen Evolution Reaction (HER).

203
204
205

The expected products of glucose oxidation and reduction, respectively gluconic acid and sorbitol, show electrochemical activity on nickel electrodes. These compounds were added to a KOH (0.1 mol L⁻¹) solution and their electrochemical activity was observed, based on the comparison of their cyclic voltammetry curve with the one of KOH solution.

206

207

208

209

210

211

212

213

214

215

216

217

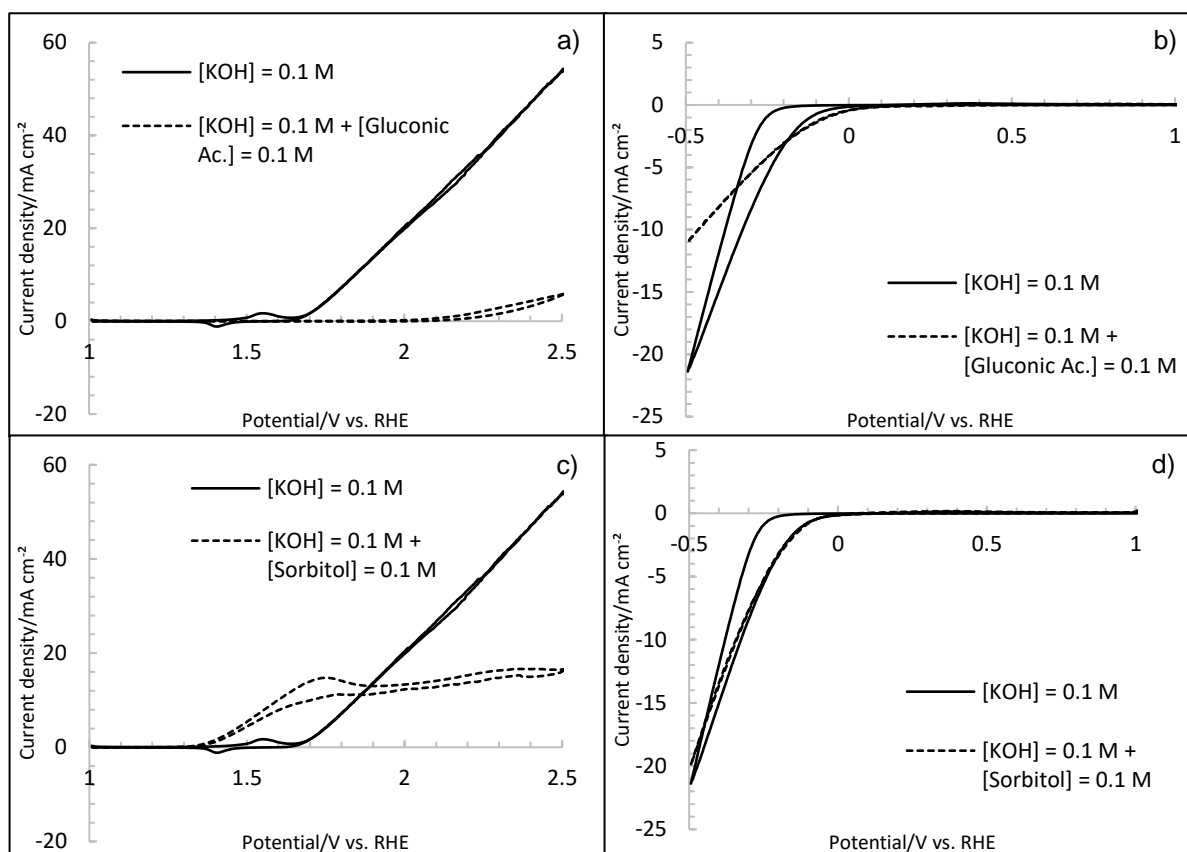


Figure 4. CV curves of gluconic acid and sorbitol with 0.1 mol L⁻¹ KOH solution at a sweep rate of 20 mV s⁻¹ on Ni foam, a) for the oxidation of gluconic acid at 0.1 mol L⁻¹ between 1 V and 2.5 V vs. RHE, b) for the reduction of gluconic acid at 0.1 mol L⁻¹ between 1 V and -0.5 V vs. RHE, c) for the oxidation of sorbitol at 0.1 mol L⁻¹ between 1 V and 2.5 V vs. RHE, d) for the reduction of sorbitol at 0.1 mol L⁻¹ between 1 V and 2.5 V vs. RHE

218

219 We observe that the electrocatalytic activity of nickel hydroxide disappears in presence of gluconic acid (Figure 4a) due to the electrode
 220 passivation. Therefore, gluconic acid might be difficult to produce on pure nickel electrode if gluconic acid passivates the electrode;
 221 gluconic acid could be desorbed from the electrode using a lower potential. However, cyclic voltammetry of gluconic acid shows that it
 222 can be reduced (Figure 4b) at the cathode. Therefore, it shows the importance to separate both anodic and cathodic compartments, to
 223 not degrade the desired products into undesired products.

224 Sorbitol has a high electrochemical activity at the anode and can be oxidised (Figure 4c). However, at the cathode, sorbitol shows no
 225 electrochemical activity (Figure 4d). Indeed, the molecular structure of sorbitol shows no organic function that can be reduced.

226 Considering that the desired products can be oxidised and reduced, it shows the importance to have a high-performance separator,
 227 such as an anion exchange membrane, to separate anodic and cathodic compartments.

228 Long-term electrolysis results

229 After 5 hours long-term electrolysis, HPLC was used to qualify and quantify the reaction products from the glucose electrooxidation
 230 and electroreduction. Side products have been identified using this analytical tool with 2 detectors: refractive index detector (Figure 5
 231 & Figure 6) and ultraviolet detector (Figure 4) and comparison with analytical grade standards.

232 Many side products have been identified in the anodic compartment due to glucose degradation on nickel electrodes: fructose as an
 233 isomerization product of glucose in alkaline medium and oxalic acid, tartronic acid, arabinose, glyceric acid, glycolic acid and formic
 234 acid as degradation products of glucose at high potential. The reverse peak observed is due to the elution of sample solvent.
 235
 236

237 With this set up, retention times can be determined for each peak and each detector.

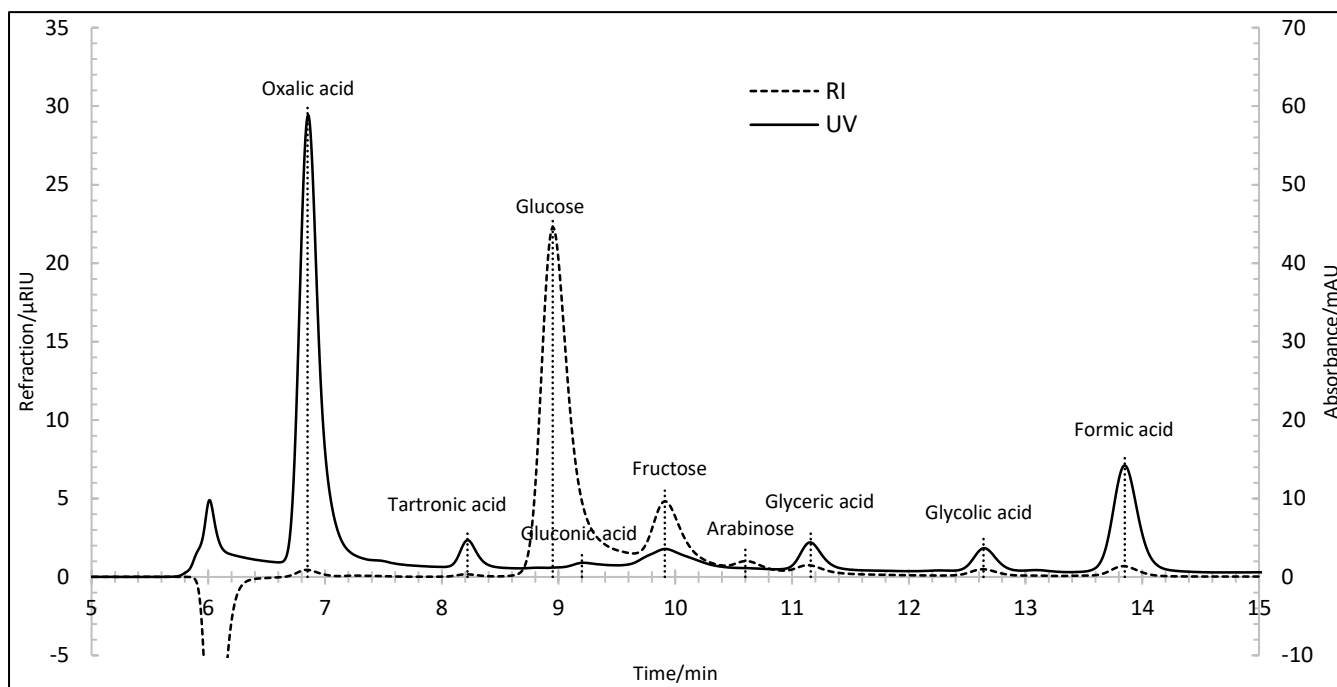


Figure 5 - Chromatogram of the anodic compartment (RID & UVD) after 5 hours of electrolysis on Ni-Co electrodes at 1.475 V vs RHE

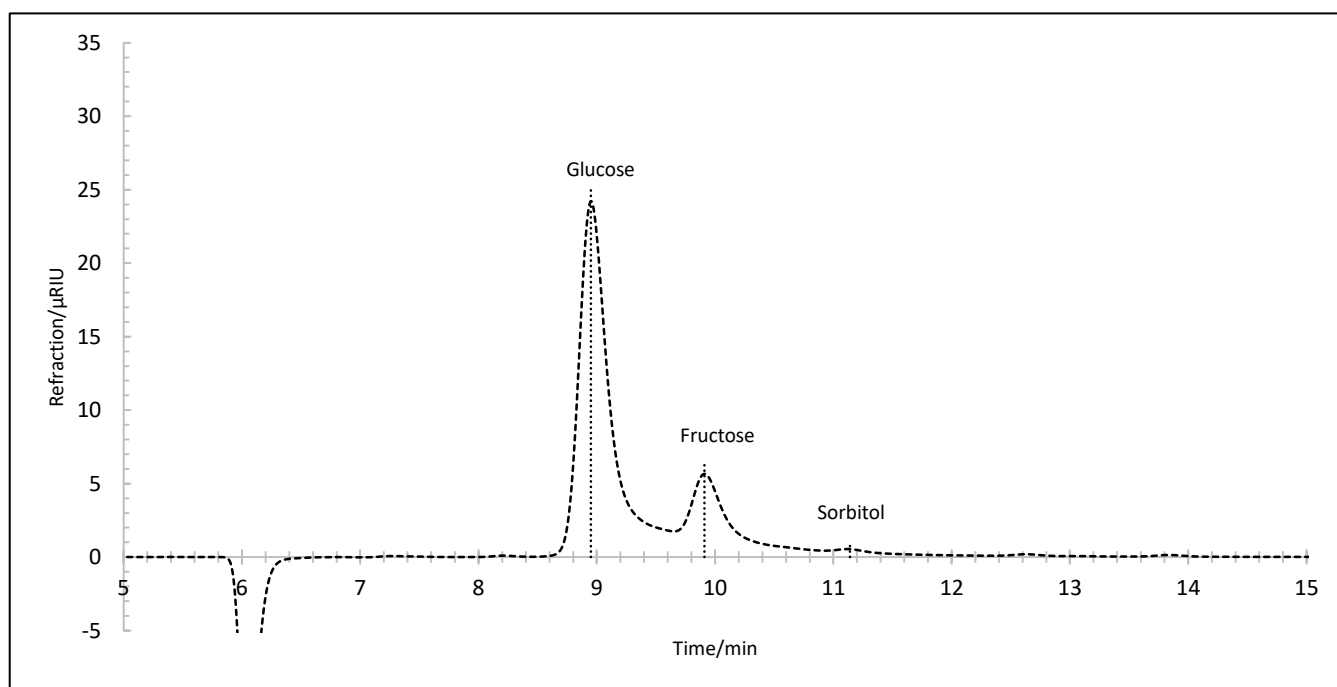


Figure 6 - Chromatogram of the cathodic compartment (RID) after 5 hours of electrolysis on Ni-Co electrodes at 1.475 V vs RHE

238

239 In order to see the performance of the electrodes with NiM bimetallic particles (Ni-Ni, Ni-Co, Ni-Rh), electrolysis have been carried out
240 under the same operating conditions in an electrochemical reactor: electrolysis time (5 hours), flow rate (100 mL min^{-1}), applied potential
241 (1.475 V vs RHE), reactant concentrations ($[\text{glucose}] = 0.028 \text{ mol L}^{-1}$ and $[\text{KOH}] = 0.1 \text{ mol L}^{-1}$). For all experiments, the electrolysis
242 solution is fully recycled. For each electrode tested, experiments were performed 3 times. Uncertainties were calculated for glucose
243 conversion, products yield, products selectivity and charge consumed.

244

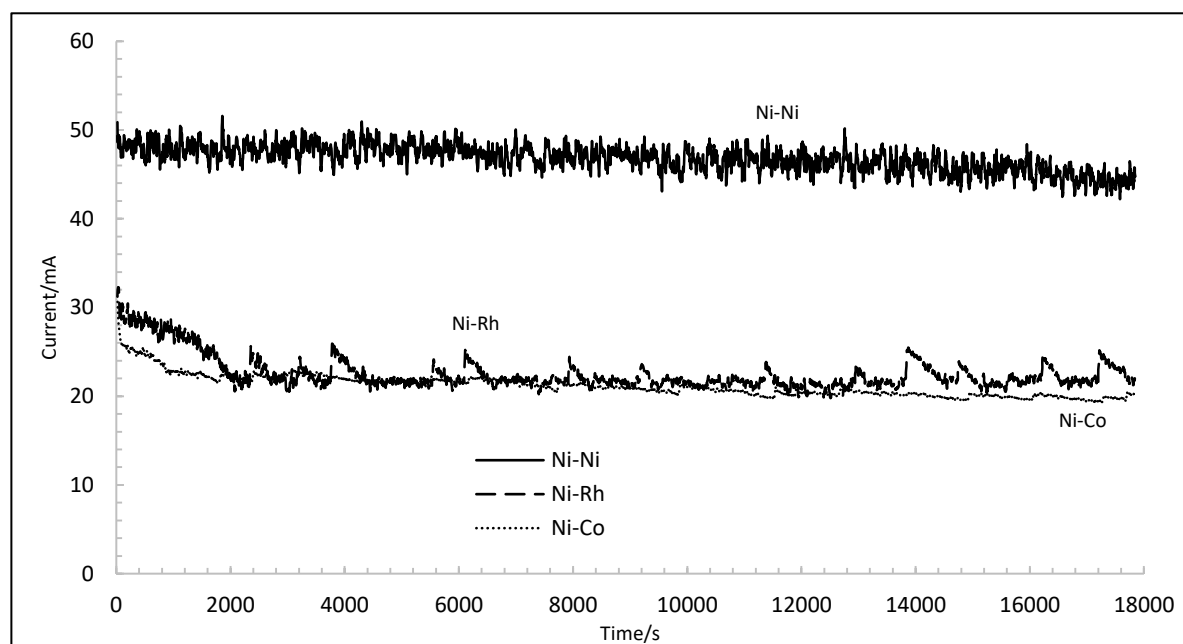


Figure 7. Chronoamperometry curve $I=f(t)$ after 5 hours electrolysis on different NiM electrodes at 1.475 V vs RHE; $[G] = 0.028 \text{ mol L}^{-1}$; $[\text{KOH}] = 0.1 \text{ mol L}^{-1}$

259 In Figure 7, chronoamperometry curves for all metals demonstrate a consistently stable current over time, with no observed electrode
260 deactivation.

261 **Table 2.** Electrolysis results for the Ni-Ni, Ni-Rh and Ni-Co electrodes (applied potential of 1.475 V vs RHE, flow rate of 100 mL min^{-1} , electrolysis length of 5 hours,
262 $[\text{glucose}] = 0.028 \text{ mol L}^{-1}$, $[\text{KOH}] = 0.1 \text{ mol L}^{-1}$): glucose conversion, gluconic acid yield and selectivity

Electrode		Ni-Ni	Ni-Rh	Ni-Co
Anode	X_G (%)	$47.9\% \pm 5\%$	$40.4\% \pm 4\%$	$42.9\% \pm 2\%$
	Y_{GA} (%)	$0\% \pm 0\%$	$0\% \pm 0\%$	$0.4\% \pm 0.1\%$
	S_{GA} (%)	$0\% \pm 0\%$	$0\% \pm 0\%$	$1\% \pm 0.3\%$
Cathode	X_G (%)	$35.2\% \pm 5\%$	$35.2\% \pm 4\%$	$37.2\% \pm 2\%$
	Y_S (%)	$0.4\% \pm 0.7\%$	$1.9\% \pm 0.5\%$	$2\% \pm 0.5\%$
	S_S (%)	$1.1\% \pm 2\%$	$5.3\% \pm 1.2\%$	$5.5\% \pm 1.3\%$
Q (C)		797 ± 120	433 ± 34	353 ± 28

263
264 The desired oxidation and reduction products from glucose (gluconic acid and sorbitol) have very low yields and selectivities with these
265 operating conditions (Table 2). Indeed, when glucose is oxidized at high voltage potential, C-C bonds can break and create degradation
266 products. Moreover, glucose in alkaline medium naturally isomerizes into fructose.

267 In addition to gluconic acid and sorbitol, several other products were detected: fructose, tartronic acid, oxalic acid, glycolic acid and
268 formic acid. HPLC detectors (RI & UV) also detected additional products that remain unidentified. Degradation products originating
269 from glucose are more likely to manifest at high voltage potential (1.475 V vs RHE) in the anodic compartment (Table 3 & Table 4).
270 Indeed, NiOH and NiO species can react with C_6 molecules, potentially causing C-C bond cleavage and subsequent degradation
271 products [35]. To prevent the formation of these degradation products, nickel electrodes with other particles that lead to lower oxidation
272 voltage potentials should be explored.

273 **Table 3.** Yield of fructose (F), arabinose (Ara), tartronic acid (Tar. Ac.), oxalic acid (Ox. Ac.), glyceric acid (Glyce. Ac.), glycolic acid (Glyco. Ac.) and formic acid
274 (For. Ac.) at the anode for the 3 electrodes tested with particles of Ni, Rh and Co

Electrode		Ni-Ni	Ni-Rh	Ni-Co
Anode	Y_F (%)	$9.6\% \pm 1\%$	$13.1\% \pm 3\%$	$14.7\% \pm 1.1\%$
	Y_{Ara} (%)	$3\% \pm 0.3\%$	$2.2\% \pm 0.7\%$	$2.6\% \pm 0.9\%$
	$Y_{Ox. Ac.}$ (%)	$0.2\% \pm 0\%$	$0.4\% \pm 0.1\%$	$0.7\% \pm 0.2\%$
	$Y_{Tar. Ac.}$ (%)	$0\% \pm 0.1\%$	$0.2\% \pm 0\%$	$0.3\% \pm 0.2\%$
	$Y_{Glyce. Ac.}$ (%)	$1.6\% \pm 0.6\%$	$0.9\% \pm 0.2\%$	$1.5\% \pm 0.2\%$
	$Y_{Glyco. Ac.}$ (%)	$2.3\% \pm 0.5\%$	$1.1\% \pm 0.3\%$	$1.2\% \pm 0.2\%$

$Y_{\text{For. Ac.}} (\%)$	$8.1\% \pm 3.5\%$	$3.5\% \pm 0.7\%$	$2.5\% \pm 0.4\%$
----------------------------	-------------------	-------------------	-------------------

Table 4. Yield of fructose (F), arabinose (Ara), tartronic acid (Tar. Ac.), oxalic acid (Ox. Ac.), glyceric acid (Glyce. Ac.), glycolic acid (Glyco. Ac.) and formic acid (For. Ac.) at the cathode for the 3 electrodes tested with particles of Ni, Rh and Co

Electrode	Ni-Ni	Ni-Rh	Ni-Co
$Y_{\text{F}} (\%)$	$14.8\% \pm 1.7\%$	$14.9\% \pm 4.2\%$	$18.3\% \pm 3.4\%$
$Y_{\text{Ara}} (\%)$	$0\% \pm 0\%$	$0\% \pm 0\%$	$0\% \pm 0\%$
$Y_{\text{Ox. Ac.}} (\%)$	$0\% \pm 0\%$	$0\% \pm 0\%$	$0\% \pm 0\%$
$Y_{\text{Tar. Ac.}} (\%)$	$0\% \pm 0.2\%$	$0.2\% \pm 0\%$	$0.2\% \pm 0\%$
$Y_{\text{Glyce. Ac.}} (\%)$	$0.4\% \pm 0.1\%$	$0.3\% \pm 0.2\%$	$0.6\% \pm 0.1\%$
$Y_{\text{Glyco. Ac.}} (\%)$	$0.3\% \pm 0.3\%$	$0.3\% \pm 0.1\%$	$0.4\% \pm 0\%$
$Y_{\text{For. Ac.}} (\%)$	$0.5\% \pm 0.4\%$	$0.3\% \pm 0.1\%$	$0.4\% \pm 0\%$

To determine the quantity of electricity consumed in electrochemical reactions, Faraday efficiency is employed to assess the efficiency of charge transfer during these reactions. Faraday efficiency has been computed not only for the primary products, such as gluconic acid and sorbitol, but also for the identified degradation products, including arabinose, oxalic acid, tartronic acid, glyceric acid, glycolic acid, and formic acid.

Table 5. Faraday efficiency of gluconic acid (GA) and sorbitol (S) for the three electrodes tested

Electrode	Ni-Ni	Ni-Rh	Ni-Co
$\varphi_{\text{GA}} (\%)$	$0\% \pm 0\%$	$0\% \pm 0\%$	$1.3\% \pm 0.7\%$
$\varphi_{\text{S}} (\%)$	$0.5\% \pm 1.8\%$	$4.7\% \pm 2\%$	$6.3\% \pm 2.8\%$

In the anodic compartment, the desired product utilizes only a small fraction of the electricity consumed by the system, as indicated in Table 5. Notably, when the Faraday efficiency of the byproducts (as presented in Table 6) is examined, a larger amount of electricity has been consumed in their formation. Specifically, formic acid formation consumes half of the electricity required for the electrochemical formation of all chemical species. This Faraday efficiency analysis reveals that these modified nickel foams are not suitable for oxidizing glucose into gluconic acid.

Table 6. Faraday efficiency of fructose (F), arabinose (Ara), tartronic acid (Tar. Ac.), oxalic acid (Ox. Ac.), glyceric acid (Glyce. Ac.), glycolic acid (Glyco. Ac.) and formic acid (For. Ac.) for the three electrodes tested

Electrode	Ni-Ni	Ni-Rh	Ni-Co
$\varphi_{\text{Ara}} (\%)$	$9.6\% \pm 2.6\%$	$13.2\% \pm 4.4\%$	$19.5\% \pm 7.4\%$
$\varphi_{\text{Ox. Ac.}} (\%)$	$2.6\% \pm 0.7\%$	$8.7\% \pm 1.7\%$	$20.2\% \pm 5.3\%$
$\varphi_{\text{Tar. Ac.}} (\%)$	$0.3\% \pm 1.2\%$	$2.4\% \pm 0.4\%$	$5.6\% \pm 3\%$
$\varphi_{\text{Glyce. Ac.}} (\%)$	$4.2\% \pm 1.8\%$	$4.3\% \pm 1.2\%$	$9.4\% \pm 1.7\%$
$\varphi_{\text{Glyco. Ac.}} (\%)$	$9.2\% \pm 2.9\%$	$8.5\% \pm 2.5\%$	$11.5\% \pm 2.2\%$
$\varphi_{\text{For. Ac.}} (\%)$	$63.5\% \pm 32.1\%$	$52.6\% \pm 12.2\%$	$47\% \pm 9.9\%$

In the cathodic compartment, the desired product utilizes a larger portion of the electricity consumed, but this portion remains relatively insignificant, as demonstrated in Table 5. Approximately 90 to 95% of the electricity consumed in the cathodic section has been allocated to another reduction reaction, most likely the reduction of water into hydrogen.

Conclusion

In summary, the incorporation of mono-/bi-metallic NiM particles onto nickel electrodes enhances their performance in facilitating the electrochemical oxidation and reduction of glucose. However, it's important to note that in basic media, the isomerization of glucose (Lobry de Bruyn – van Ekenstein reaction) into fructose is catalyzed [36]. Additionally, when applying a high potential to nickel electrodes with particles for the electrooxidation of glucose, side products emerge due to the breaking of C-C bonds (resulting in oxalic, tartronic, glycolic, formic acids, and others). Using these modified nickel electrodes with Ni-Ni, Ni-Rh, and Ni-Co, achieving successful electrooxidation and electroreduction of glucose proves challenging and leads to very low yields and selectivities towards gluconic acid and sorbitol.

305 Given that a significant portion of electricity is consumed in degrading glucose into numerous carboxylic acids, it becomes apparent
306 that alternative particle materials should be explored to enhance electrooxidation and electroreduction yields and selectivities. This
307 pursuit aims to produce gluconic acid and sorbitol more efficiently.

308 **Keywords:** glucose • long-term electrolysis • nickel • gluconic acid • sorbitol

309 References

- 310 [1] T. Werpy, G. Petersen, *Energy Efficiency and Renewable Energy, Volume 1*, 2004.
- 311 [2] European Commission Directorate-General Energy, 2015, N° ENER/C2/423-2012/SI2.673791.
- 312 [3] K. Ahuja, S. Singh, *Gluconic Acid Market by Application, by Downstream Potential, Regional Outlook, Application Potential, Price Trend, Competitive Market*
313 *Share & Forecast, 2018–2024*. Selbyville, DE: Global Market Insights Inc, 240, 2018.
- 314 [4] C. Marques, R. Tarek, M. Sara, S.K. Brar, *Sorbitol Production From Biomass and Its Global Market, Platform Chemical Biorefinery*, 2016.
- 315 [5] H. Hustede, H.-J. Haberstroh., E. Schinzig, *Ullmann's Encyclopedia of Industrial Chemistry*, 7th ed., 2007.
- 316 [6] M. J. Climent, A. Corma, S. Iborra, *Green Chem*, 2011, 13, 520-540.
- 317 [7] D. S. P. Cardoso, B. Šljukić, D. M. F. Santos, C. A. C. Sequeira, *Org. Process Res. Dev.*, 2017, 21, 1213-1226.
- 318 [8] F. W. S. Lucas, R. Gary Grim, S. A. Tacey, C. A. Downes, J. Hasse, A. M. Roman, C. A. Farberow, J. A. Schaidle, A. Holewinski, *ACS Energy Lett.* 2021, 6,
319 1205– 1270.
- 320 [9] P. Prabhu, Y. Wan, J.-M. Lee, *Matter* 2020, 3, 1162 – 1177.
- 321 [10] B. J. Taitt, D.-H. Nam, K.-S. Choi, *ACS Catal.* 2019, 9, 660 – 670.
- 322 [11] R. Latsuzbaia, R. Bisselink, A. Anastasopol, H. van der Meer, R. van Heck, M. Segurola Yagüe, M. Zijlstra, M. Roelands, M. Crockatt, E. Goetheer, E. Giling,
323 *J. Appl. Electrochem* 2018, 48, 611 – 626.
- 324 [12] C. Dai, L. Sun, H. Liao, B. Khezri, R. D. Webster, A. C. Fisher, Z. J. Xu, *Journal of Catalysis* 2017, 356, 14 – 21.
- 325 [13] A. Talebian-Kiakalaieh, N. A. S. Amin, K. Rajaei, S. Tarighi, *Applied Energy* 2018, 230, 1347 – 1379.
- 326 [14] Y. Qiu, L. Xin, D. J. Chadderdon, J. Qi, C. Liang, W. Li, *Green Chem* 2014, 16, 1305 – 1315.
- 327 [15] T. R. dos Santos, P. Nilges, W. Sauter, F. Harnisch, U. Schroder, *RSC Adv.* 2015, 5, 26634 – 26643.
- 328 [16] A.T. Governo, L. Proença, P. Parpot, M.I.S. Lopes, I.T.E. Fonseca, *Electrochim. Acta* 49 (2004) 1535–1545.
- 329 [17] T. Rafaïdeen, S. Baranton, C. Coutanceau. *Appl. Catal. B: Env.* 243 (2019) 641–656.
- 330 [18] N Neha, T. Rafaïdeen, T. Faverge, F. Maillard, M. Chatenet, C. Coutanceau. *Electrocatalysis* 14 (2023) 121-130.
- 331 [19] T. Faverge, B. Gilles, A. Bonnefont, F. Maillard, C. Coutanceau, M. Chatenet. *ACS Catal.* 13 (2023) 2657–2669.
- 332 [20] G. Sanghez de Luna, P. H. Ho, A. Sacco, S. Hernandez, J.-J. Velasco-Vélez, F. Ospitali, A. Paglianti, S. Albonetti, G. Fornasari, P. Benito, *ACS Appl. Mater*
333 *Interfaces* 2021, 13, 23675 – 23688.
- 334 [21] T. Lund, H. Lund, *Acta Chemica Scandinavica B* 1985, 39, 429 – 435.
- 335 [22] A. J. Rudge, *Industrial Electrochemical Processes*, ed. A. T. Kuhn, Elsevier Publishers, Amsterdam, London, New York, 1971.
- 336 [23] K. Li, Y. Sun, *Chem. Eur. J.* 2018, 24, 18258-18270
- 337 [24] S. Möhle, M. Zirbes, E. Rodrigo, T. Gieshoff, A. Wiebe, S. R. Waldvogel, *Angew.Chem.Int.Ed.* 2018, 57,6018–6041.
- 338 [25] P. N. Pintauro, D. K. Johnson, K. Park, M. M. Baizer, K. Nobe, *J. Appl. Electrochem.*, 1984, 14, 209-220.
- 339 [26] K. Park, P. N. Pintauro, M. M. Baizer, K. Nobe, *J. Electrochem. Soc.*, 1985, 132, 1850-1855.
- 340 [27] G. Moggia, T. Kenis, N. Daems, T. Breugelmans, *ChemElectroChem* 2020, 7, 86-95.
- 341 [28] T. Faverge, B. Gilles, A. Bonnefont, F. Maillard, C. Coutanceau, M. Chatenet, *ACS Catal* 2023, 13, 2657 – 2669.
- 342 [29] M. Bonomo, *J. Nanopart. Res.*, 2018, 20, 222.
- 343 [30] D. Wang, W. Yan, S. H. Vijapur, G. G. Botte, *Journal of Power Sources*, 2012, 217, 498-502.
- 344 [31] A. Schranck, R. Marks, E. Yates, K. Doudrick, *Environ. Sci. Technol.* 2018, 52, 15, 8638–8648.
- 345 [32] M.-S. Wu, G.-W. Lin, R.-S. Yang, *Journal of Power Sources*, 2014, 272, 711-718.
- 346 [33] S. De Los Santos Meran, *PhD thesis, INSA Rouen*, 2021.
- 347 [34] Norme NF ISO 11352:2013 : Qualité de l'eau – Estimation de l'incertitude de mesure basée sur des données de validation et de contrôle qualité.
- 348 [35] V. Vedovato, K. Vanbroekhoven, D. Pant, J., Helsen, *Molecules*, 2020, 25, 3712.
- 349 [36] F. W. Lichtenthaler, *Carbohydrates: Occurrence, Structures and Chemistry. Ullmann's Encyclopedia of Industrial Chemistry*, 2010, 1-3

